

ABSTRACT

There are several sources of mechanical compliance in a multiple degree of freedom manipulator, e.g., link flexibility, the actuators' internal characteristics and transmission mechanisms. In this work, the last case is considered. We study a two-link manipulator using a dc servo motor on each link to control the torque transmitted to the links via elastic cables. The effects of actuator dynamics and cable elasticities on the dynamics of the manipulator are examined. Based on a displacement control strategy, general conditions of local stability for the closed loop system are obtained. We also develop a simulation model for the manipulator. The obtained results should provide a framework for further study of control of cable driven manipulators.

TABLE OF CONTENTS

1. INTRODUCTION	3
1.1. Problem Description	3
1.2. Outline of the Report	3
2. MODELLING THE MANIPULATORS	3
2.1. Geometry of Manipulator	3
2.2. CASE I Manipulator Model	10
2.3. CASE II Manipulator Model	10
2.4. CASE III Manipulator Model	11
2.5. CASE IV Manipulator Model	11
3. FINAL-POSITION CONTROL	11
3.1. The Control Law	11
3.2. CASE I Closed Loop Model	13
3.3. CASE II Closed Loop Model	13
3.4. CASE III Closed Loop Model	14
3.5. CASE IV Closed Loop Model	15
3.6. Simulation Results	16
4. CONCLUSIONS	24
4.1. Summary	24
4.2. Future Work	24
5. APPENDIX	25
6. REFERENCES	26

1. INTRODUCTION

1.1. Problem Description

In this report, we consider a simple two link mechanical manipulator to emulate, in part, the human biceps/triceps system for moving the arm. The manipulator consists of two rigid links, two tendon cables and two springs. Movement of the links are made possible by two tendon cables: one end of each tendon cable is attached to the end of each link and the other end is wound on a DC servo motor shaft. The servo motors with attached cables simulate the agonists and the elastic springs simulate the antagonist muscles. By controlling the voltage input of the motors, these two links can be caused to move in a plane. The detailed description of the manipulator configuration is given in section 2.1.

Our objective is to carefully analyze the influences of the motor inductances and cable elasticities on the motion of the manipulator. The elastic cables provide some flexible compliance to the manipulator, which may prove useful for achieving certain manufacturing tasks and for safety reasons. A similar cable-driven manipulator was proposed by Riemenschneider et al [1]; Lim [2] also used the same strategy but for a different mechanical system. However, they didn't handle the cable elasticities and actuator dynamics completely.

Since the equations of motion of the manipulator are highly nonlinear and complicated, we focus on developing mathematical models of the open-loop manipulator under various assumptions. For control purpose we consider simple displacement feedback of links to regulate the motion.

1.2. Outline of the Report

This report is organized into four chapters: Chapter 1 is the introduction. Chapter 2 describes the physical mechanical manipulator and develops a mathematical model. We consider four cases: inelastic cables ignoring motor inductances effects; inelastic cables including motor inductances effects; elastic cables ignoring motor inductances effects; and elastic cables including motor inductances effects. The first case corresponds to the usual assumption made in the published literatures; the last case corresponds to the most comprehensive model. Chapter 3 presents the closed-loop control strategy; stability considerations and simulation results are also presented. Chapter 4 summarizes the effects of the cable elasticities and motor inductances. Finally, suggestions for future work are mentioned.

2. MODELLING THE MANIPULATORS

In order to study and develop a control strategy for the tendon arm manipulator, we first develop a mathematical model. In this chapter, the physical manipulator and the derivations of the equations describing the system dynamics are described. We consider four cases corresponding to four sets of assumptions.

2.1. Geometry of Manipulator

A schematic illustration of the manipulator configuration is shown in Figure 2.1; and Figure 2.2 indicates the geometrical relationships. Note that the first motor is mounted on the base plate; however, the second motor is located at the end of the first link. Link 1 is controlled by the first motor through tendon 1 and spring 1; Link 2 is controlled by the second motor through tendon 2

and spring 2.

Geometry

The nature of the link geometry is very complicated. Some useful geometric relations are given in the following equations: (we assume that the width of the links can be ignored.)

$$l_{a1} = (q_a^2 + r_a^2 + 2q_a r_a \cos\psi_1)^{\frac{1}{2}} \quad (2.1)$$

$$l_{a2} = (q_a^2 + r_a^2 - 2q_a r_a \cos\psi_1)^{\frac{1}{2}} \quad (2.2)$$

$$l_{b1} = [d^2 + r_b^2 - 2dr_b \cos(\psi_1 - \psi_2)]^{\frac{1}{2}} \quad (2.3)$$

$$l_{b2} = [d^2 + r_b^2 + 2dr_b \cos(\psi_1 - \psi_2)]^{\frac{1}{2}} \quad (2.4)$$

$$\sin\beta_1 = \frac{q_a \sin\psi_1}{l_{a1}} \quad (2.5)$$

$$\sin\beta_2 = \frac{q_a \sin\psi_1}{l_{a2}} \quad (2.6)$$

$$\sin\beta_3 = \frac{d \sin(\psi - \psi_2)}{l_{b1}} \quad (2.7)$$

$$\sin\beta_4 = \frac{d \sin(\psi_1 - \psi_2)}{l_{b2}} \quad (2.8)$$

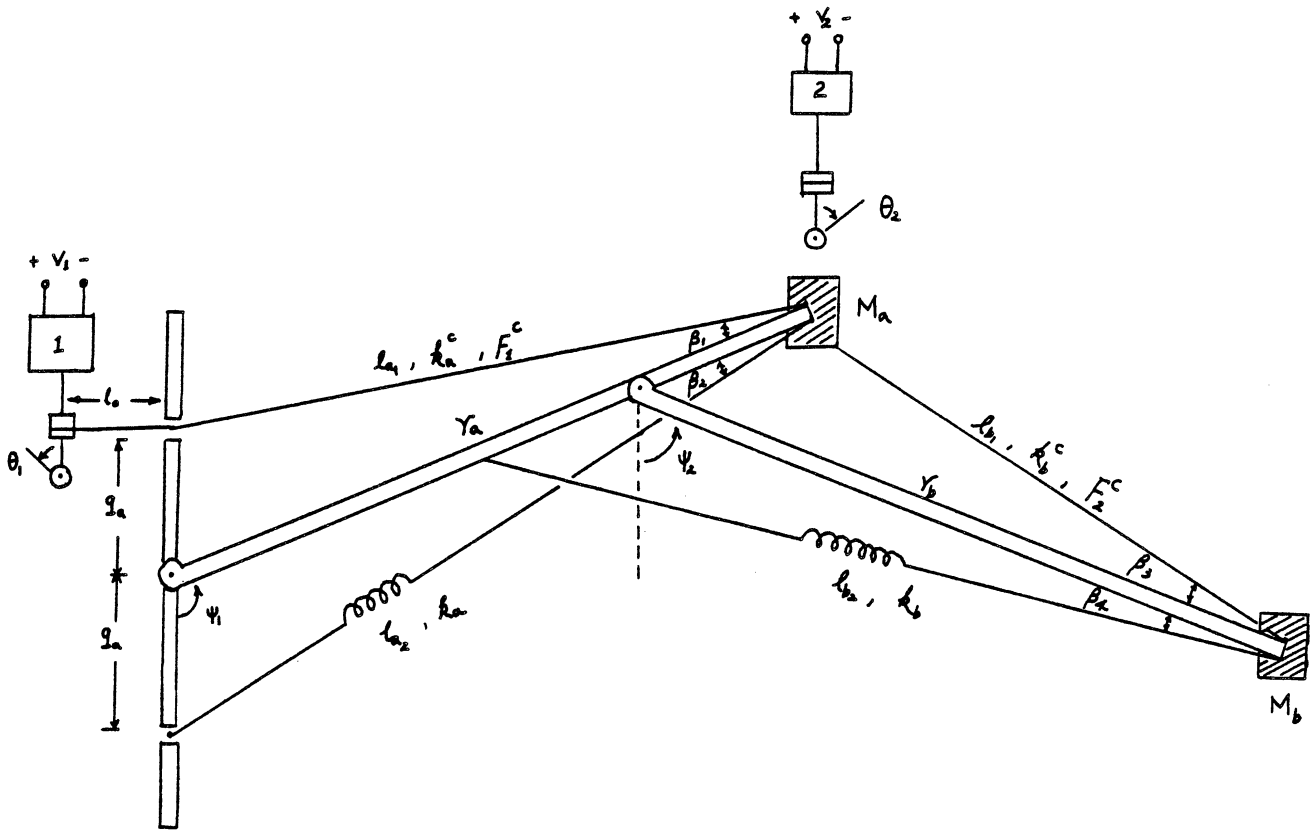


Fig 2.1 Configuration of the Tendon Arm System

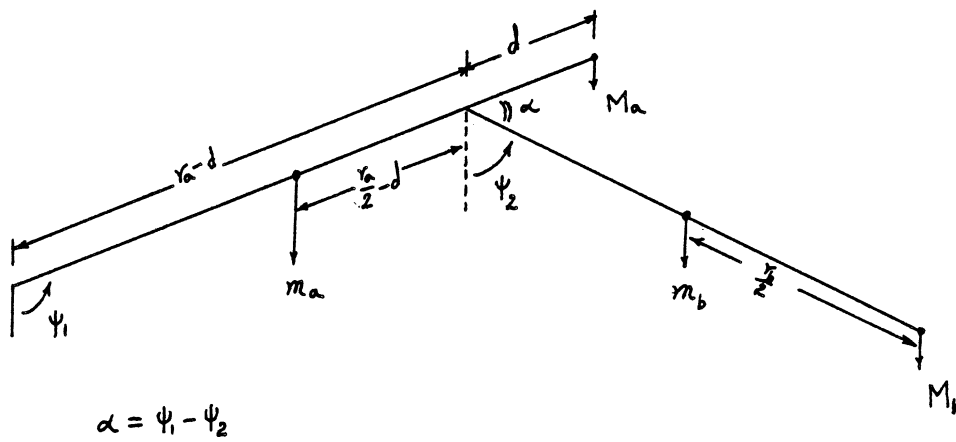


Fig 2.2 Geometric Relationship

Nomenclature

Ψ	link angle vector
Θ	shaft angle vector
L	motor inductance matrix
R	motor resistance matrix
$M(\Psi)$	inertia matrix of links
N	inertia matrix of motor shafts
F^c	cable force vector
K^c	cable stiffness matrix
$\Lambda(\Psi)$	length constraint
$J(\Psi)$	Jacobian of $\Lambda(\Psi)$
K_m	motor constraint matrix
v_1, v_2	input voltages to motor 1 & 2 (volts)
i_1, i_2	armature currents of servo motor 1 & 2 (amperes)
ϑ_1, ϑ_2	shaft angles of motor 1 & 2 (amperes)
ψ_1, ψ_2	link angles measure from the vertical (radians)
ϑ_0	initial tendon winding angles (radians)
$\alpha, \beta_1, \beta_2, \beta_3, \beta_4$	auxiliary angles (radians)
L_m	armature inductance (Henries)
R_m	armature resistances (ohms)
J_m	moment of inertia of motor shaft ($Kg - m^2$)
K_m	motor constraint ($N - m / ampere$)
r_m	pulley radius (m)
F_1^c, F_2^c	forces along the tendon cables (nt)
l_{a1}, l_{b1}	lengths of tendon cables 1 & 2 (m)
l_{a2}, l_{b2}	lengths of springs 1 & 2 (m)

$\bar{l}_{a1}, \bar{l}_{b1}$	lengths of tendon cables 1 & 2 with spring lengths \bar{l}_{a2} & \bar{l}_{b2} (m)
$\bar{l}_{a2}, \bar{l}_{b2}$	unstretched lengths of spring 1 & 2 (m)
l_0	distance from motor 1 to guide (m)
$l_{a1}^*, l_{a2}^*, l_{b1}^*, l_{b2}^*$	lengths of tendon cables and springs at equilibrium (m)
k_a, k_b	spring stiffness constants (nt/m)
k_a^c, k_b^c	elastic constants of cables 1 & 2 (nt/m)
r_a, r_b	lengths of links (m)
q_a, d	offset of guides at base of links 1 & 2 (m)

Link Dynamics

The equations of motion of the two link manipulator can be derived from a Lagrangian approach. The resultant equations of motion for the two links are

$$\begin{aligned}
& \ddot{\psi}_1 \left[\left(\frac{1}{4} m_a + M_a \right) r_a^2 + (m_b + M_b) (r_a - d)^2 \right] + \ddot{\psi}_2 \left(\frac{1}{2} m_b + M_b \right) (r_a - d) \\
& r_b \cos(\psi_1 - \psi_2) + (\dot{\psi}_2)^2 \left(\frac{1}{2} m_b + M_b \right) (r_a - d) r_b \sin(\psi_1 - \psi_2) + \left[\left(\frac{1}{2} m_a + M_a \right) g r_a \right. \\
& \left. + \left[\left(\frac{1}{2} m_a + M_a \right) g r_a + (m_a + M_b) g (r_a - d) \right] \sin \psi_1 + k_a q_a r_a \left(1 - \frac{\bar{l}_{a2}}{l_{a2}} \right) \sin \psi_1 \right. \\
& \left. - k_b d r_b \left(1 - \frac{\bar{l}_{b2}}{l_{b2}} \right) \sin(\psi_1 - \psi_2) = F_1^c \frac{q_a r_a \sin \psi_1}{l_{a1}} - F_2^c \frac{d r_b \sin(\psi_1 - \psi_2)}{l_{b1}} \right] \quad (2.9) \\
& \ddot{\psi}_2 \left(\frac{1}{4} m_b r_b^2 + M_b r_b^2 \right) + \ddot{\psi}_1 \left(\frac{1}{2} m_b + M_b \right) (r_a - d) r_b \cos(\psi_1 - \psi_2) \\
& - (\dot{\psi}_1)^2 \left(\frac{1}{2} m_b + M_b \right) (r_a - d) r_b \sin(\psi_1 - \psi_2) \\
& + \left(\frac{1}{2} m_b g r_b + M_b g r_b \right) \sin \psi_2 + k_b d r_b \left(1 - \frac{\bar{l}_{b2}}{l_{b2}} \right) \sin(\psi_1 - \psi_2)
\end{aligned}$$

$$= F_2^c \frac{dr_b \sin(\psi_1 - \psi_2)}{l_{b1}} \quad (2.10)$$

The right hand sides of these equations represent the torques applied to the links through cable forces F_1^c and F_2^c . If we denote

$$\Psi = \begin{bmatrix} \psi_1 \\ \psi_2 \end{bmatrix}, \quad \mathbf{F}^c = \begin{bmatrix} F_1^c \\ F_2^c \end{bmatrix}$$

then the equations of motion can be written as

$$\mathbf{M}(\Psi)\ddot{\Psi} + \mathbf{G}(\Psi, \dot{\Psi}) = [\mathbf{J}(\Psi)]^T \mathbf{F}^c \quad (2.11)$$

where

$$\mathbf{M}(\Psi) = \begin{bmatrix} m_{11}(\Psi) & m_{12}(\Psi) \\ m_{21}(\Psi) & m_{22}(\Psi) \end{bmatrix}, \quad \mathbf{G}(\Psi, \dot{\Psi}) = \begin{bmatrix} g_1(\Psi, \dot{\Psi}) \\ g_2(\Psi, \dot{\Psi}) \end{bmatrix}$$

$$\Lambda(\Psi) = \begin{bmatrix} l_{a1} - \bar{l}_{a1} \\ l_{b1} - \bar{l}_{b1} \end{bmatrix}$$

$$m_{11}(\Psi) = \left(\frac{1}{4}m_a + M_a\right)r_a^2 + (m_b + M_b)(r_a - d)^2$$

$$m_{12}(\Psi) = m_{21}(\Psi) = \left(\frac{1}{2}m_b + M_b\right)(r_a - d)r_b \cos(\psi_1 - \psi_2) \quad (2.12)$$

$$m_{22}(\Psi) = \frac{1}{4}m_b r_b^2 + M_b r_b^2$$

$$g_1(\Psi, \dot{\Psi}) = (\dot{\Psi}_2)^2 \left(\frac{1}{2}m_b + M_b\right)(r_a - d)r_b \sin(\psi_1 - \psi_2)$$

$$+ \left[\left(\frac{1}{2}m_a + M_a\right)gr_a + (m_b + M_b)g(r_a - d)\right] \sin\psi_1$$

$$+ k_a g_a r_a \left(1 - \frac{\bar{l}_{a2}}{l_{a2}}\right) \sin\psi_1 - k_b d r_b \left(1 - \frac{\bar{l}_{b2}}{l_{b2}}\right) \sin(\psi_1 - \psi_2) \quad (2.13)$$

$$g_2(\Psi, \dot{\Psi}) = -(\dot{\Psi}_1)^2 \left(\frac{1}{2}m_b + M_b\right)(r_a - d)r_b \sin(\psi_1 - \psi_2)$$

$$+ \left(\frac{1}{2}m_b g r_b + M_b g r_b\right) \sin\psi_2 + k_b d r_b \left(1 - \frac{\bar{l}_{b2}}{l_{b2}}\right) \sin(\psi_1 - \psi_2)$$

$[\mathbf{J}(\Psi)]^T = \text{the transpose of Jacobian of } \Lambda(\Psi)$

Motor Dynamics

A standard linear model of a DC armature-driven servo motor is used [11]. The armature circuits are described by

$$L_m \frac{di_j}{dt} + R_m i_j + K_m \frac{d\vartheta_j}{dt} = V_j ; i = 1, 2 \quad (2.14)$$

Euler's equations for the motor shafts are

$$J_m \frac{d^2\vartheta_j}{dt^2} = K_m i_j - r_m F_j^c ; i = 1, 2 \quad (2.15)$$

The parameters of both motors are assumed to be identical. Again if we write

$$\Theta = \begin{bmatrix} \vartheta_1 \\ \vartheta_2 \end{bmatrix}, \quad z = \begin{bmatrix} i_1 \\ i_2 \end{bmatrix}, \quad u = \begin{bmatrix} v_1 \\ v_2 \end{bmatrix}$$

then the above two equations become

$$\mathbf{L}\dot{z} = -\mathbf{R}z - \mathbf{K}_m \dot{\Theta} + u \quad (2.16)$$

$$\mathbf{N}\ddot{\Theta} = \mathbf{K}_m z - r_m \mathbf{F}^c \quad (2.17)$$

where

$$\mathbf{L} = \begin{bmatrix} L_m & 0 \\ 0 & L_m \end{bmatrix}, \quad \mathbf{R} = \begin{bmatrix} R_m & 0 \\ 0 & R_m \end{bmatrix}, \quad \mathbf{K}_m = \begin{bmatrix} K_m & 0 \\ 0 & K_m \end{bmatrix}$$

$$\mathbf{N} = \begin{bmatrix} J_m & 0 \\ 0 & J_m \end{bmatrix}$$

Cable Constraints

Force constraints, if the cables are assumed to be elastic, are given by

$$\mathbf{F}^c = \mathbf{K}^c [r_m \Theta - \Lambda(\Psi)] \quad (2.18)$$

Holonomic constraints, if the cables are assumed to be inelastic, are given by

$$r_m \Theta - \Lambda(\Psi) = 0 \quad (2.19)$$

where

$$\mathbf{K}^c = \begin{bmatrix} k_a^c & 0 \\ 0 & k_b^c \end{bmatrix}$$

In the following, mathematical models are developed for four cases indicated.

2.2. CASE I Manipulator Model

We start with the simplest case -- where the tendon cables are assumed to be inelastic and motor inductance effects are ignored. This case has been widely applied in most robot control designs [1-5].

>From the holonomic constraints (2.19) we have

$$\begin{aligned}\Theta &= \frac{1}{r_m} \Lambda(\Psi) \\ \dot{\Theta} &= \frac{1}{r_m} \mathbf{J}(\Psi) \dot{\Psi} \\ \ddot{\Theta} &= \frac{1}{r_m} \mathbf{J}(\Psi) \ddot{\Psi} + \frac{1}{r_m} \frac{d}{dt} [\mathbf{J}(\Psi)] \dot{\Psi}\end{aligned}\quad (2.20)$$

Usually motor inductances are quite small; if they are ignored, (2.16) reduces to

$$\mathbf{z} = -\mathbf{R}^{-1} \mathbf{K}_m \dot{\Theta} + \mathbf{R}^{-1} \mathbf{u} \quad (2.21)$$

Substituting (2.20) and (2.21) into (2.17), we obtain

$$\mathbf{F}^c = \frac{-1}{r_m^2} \mathbf{N} \mathbf{J}(\Psi) \ddot{\Psi} - \frac{1}{r_m^2} \left\{ \mathbf{N} \frac{d}{dt} [\mathbf{J}(\Psi)] + \mathbf{K}_m \mathbf{R}^{-1} \mathbf{K}_m \mathbf{J}(\Psi) \right\} \dot{\Psi} + \frac{1}{r_m} \mathbf{K}_m \mathbf{R}^{-1} \mathbf{u} \quad (2.22)$$

Thus the equations of motion are

$$\begin{aligned}\{\mathbf{M}(\Psi) + [\mathbf{J}(\Psi)]^T \frac{\mathbf{N}}{r_m^2} \mathbf{J}(\Psi)\} \ddot{\Psi} + \mathbf{G}(\Psi, \dot{\Psi}) + [\mathbf{J}(\Psi)]^T \frac{\mathbf{N}}{r_m^2} \frac{d}{dt} [\mathbf{J}(\Psi)] \dot{\Psi} \\ + [\mathbf{J}(\Psi)]^T \frac{\mathbf{K}_m \mathbf{R}^{-1} \mathbf{K}_m}{r_m^2} \mathbf{J}(\Psi) \dot{\Psi} = [\mathbf{J}(\Psi)]^T \frac{\mathbf{K}_m \mathbf{R}^{-1}}{r_m} \mathbf{u}\end{aligned}\quad (2.23)$$

where $\mathbf{M}(\Psi)$ and $\mathbf{G}(\Psi, \dot{\Psi})$ are defined in (2.12) and (2.13). Note that the effective inertia matrix is symmetric and positive definite for all Ψ .

2.3. CASE II Manipulator Model

The assumptions are the same as for CASE I except that the motor inductances are included in the analysis. Using (2.20) and (2.17) in (2.16), (2.11), we obtain

$$\{\mathbf{M}(\Psi) + [\mathbf{J}(\Psi)]^T \frac{\mathbf{N}}{r_m^2} \mathbf{J}(\Psi)\} \ddot{\Psi} + \{\mathbf{G}(\Psi, \dot{\Psi})\} \quad (2.24)$$

$$+ [\mathbf{J}(\Psi)]^T \frac{\mathbf{N}}{r_m^2} \frac{d}{dt} [\mathbf{J}(\Psi)] \dot{\Psi} = [\mathbf{J}(\Psi)]^T \frac{\mathbf{K}_m}{r_m} \mathbf{z}$$

$$\mathbf{L} \dot{\mathbf{z}} = -\mathbf{R} \mathbf{z} - \frac{\mathbf{K}_m}{r_m} [\mathbf{J}(\Psi)] \dot{\Psi} + \mathbf{u} \quad (2.25)$$

Eqs. (2.24), (2.25) describe the arm system driven by inelastic cables. Obviously, in this case four variables $(\psi_1, \psi_2, i_1, i_2)$ are required instead of two, as in CASE I, to describe the manipulator. The additional two variables are due to the effects of motor dynamics. Clearly, if $L = 0$ the model developed in this case reduces to the model given for CASE I.

2.4. CASE III Manipulator Model

Next we extend our development to a more general case. The cables are assumed to be elastic with stiffness constants k_a^c and k_b^c respectively.

Hence the equations of motion can be obtained

$$\begin{bmatrix} \mathbf{M}(\Psi) & 0 \\ 0 & \mathbf{N} \end{bmatrix} \begin{bmatrix} \ddot{\Psi} \\ \ddot{\Theta} \end{bmatrix} + \begin{bmatrix} \mathbf{G}(\Psi, \dot{\Psi}) - \tau_m [\mathbf{J}(\Psi)]^T \mathbf{K}^c \Theta + [\mathbf{J}(\Psi)]^T \mathbf{K}^c \Lambda(\Psi) \\ \mathbf{K}_m \mathbf{R}^{-1} \mathbf{K}_m \Theta + \tau_m^2 \mathbf{K}^c \Theta - \tau_m \mathbf{K}^c \Lambda(\Psi) \end{bmatrix} \quad (2.26)$$

$$= \begin{bmatrix} 0 \\ \mathbf{K}_m \mathbf{R}^{-1} \end{bmatrix} u$$

where the force constraint (2.18) and (2.21) are used in eqs (2.11) and (2.17).

2.5. CASE IV Manipulator Model

Finally, we examine the most general case -- the cables are elastic and the motor inductances are included. This case is more complicated than the other cases although it can fully describe the tendon manipulator.

>From eqs (2.11), (2.16), (2.17), (2.18) the equations of motion are obtained as follows:

$$\begin{bmatrix} \mathbf{M}(\Psi) & 0 \\ 0 & \mathbf{N} \end{bmatrix} \begin{bmatrix} \ddot{\Psi} \\ \ddot{\Theta} \end{bmatrix} + \begin{bmatrix} \mathbf{G}(\Psi, \dot{\Psi}) - [\mathbf{J}(\Psi)]^T \mathbf{K}^c [\tau_m \Theta - \Lambda(\Psi)] \\ \tau_m^2 \mathbf{K}^c \Theta - \tau_m \mathbf{K}^c \Lambda(\Psi) \end{bmatrix}$$

$$= \begin{bmatrix} 0 \\ \mathbf{K}_m \end{bmatrix} z \quad (2.27)$$

$$\mathbf{L} \dot{z} = -\mathbf{R}z - \mathbf{K}_m \dot{\Theta} + u$$

>From the above formulations of the equations of motion, we infer that even for higher degree of freedom cable driven systems the equations of motion will have the same forms as described in this chapter.

3. FINAL-POSITION CONTROL

3.1. The Control Law

Since one joint of the link system is attached to the base guide and the other joint is attached to the first link, positive steady-state tensions in the tendon cables are required to maintain the link at any specified final position. The required control voltages can be calculated by examination of the equilibrium conditions. Our control objective is to bring the joint angle vector Ψ to

the desired final setting Ψ^* and to maintain them there, that is,

$$\Psi(t) \rightarrow \Psi^* \quad \text{as } t \rightarrow \infty$$

A linear feedback controller based on feedback of the angular velocities $\dot{\Theta}$ of the motor shafts is suggested. The detailed control structure is shown in Fig. 3.1, and the control law is given by

$$u = u^* - H\dot{\Theta} \tag{3.1}$$

where u^* is a constant value determined to maintain the manipulator in equilibrium, and

$$H = \begin{bmatrix} h_1 & 0 \\ 0 & h_2 \end{bmatrix}$$

is a feedback gain matrix.

This simple feedback control law is commonly employed in conventional manipulator control design [4,5], because it is easily implemented as well as easily tuned to stabilize the closed loop.

In the following four cases, corresponding to the assumptions indicated previously, we show how to determine u^* in terms of Ψ^* . Both nonlinear and linearized closed loop equations are developed, and simple conditions for local stability of the closed loop system are obtained.

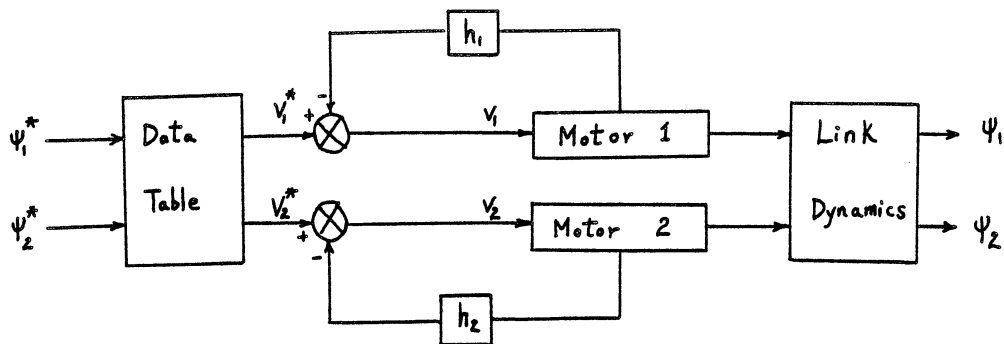


Fig 3.1 Control Structure

3.2. CASE I Closed Loop Model

Suppose that it is desired that the manipulator be in equilibrium when $\Psi = \Psi^*$. Then from eq. (2.23) it follows that $u = u^*$ must satisfy

$$\mathbf{G}(\Psi^*, 0) = [\mathbf{J}(\Psi^*)]^T \frac{\mathbf{K}_m \mathbf{R}^{-1}}{r_m} u^* \quad (3.2)$$

The calculation of u^* in terms of Ψ^* defines a so-called data table or feedforward control.

Now the closed-loop equations, based on eq. (2.23) and (3.1), can be written as

$$\begin{aligned} \{\mathbf{M}(\Psi) + [\mathbf{J}(\Psi)]^T \frac{\mathbf{N}}{r_m^2} \mathbf{J}(\Psi)\} \ddot{\Psi} + \{\mathbf{G}(\Psi, \dot{\Psi}) + [\mathbf{J}(\Psi)]^T \frac{\mathbf{N}}{r_m^2} \frac{d}{dt} [\mathbf{J}(\Psi)] \dot{\Psi} \\ + [\mathbf{J}(\Psi)]^T \frac{\mathbf{K}_m \mathbf{R}^{-1} \mathbf{K}_m}{r_m^2} \mathbf{J}(\Psi) \dot{\Psi} + [\mathbf{J}(\Psi)]^T \frac{\mathbf{K}_m \mathbf{R}^{-1} \mathbf{H}}{r_m^2} \mathbf{J}(\Psi) \dot{\Psi}\} = [\mathbf{J}(\Psi)]^T \frac{\mathbf{K}_m \mathbf{R}^{-1}}{r_m} u^* \end{aligned} \quad (3.3)$$

If we define

$$\Psi = \Psi^* + \delta\Psi$$

then the linear perturbational equations can be obtained as

$$\begin{aligned} \{\mathbf{M}(\Psi^*) + [\mathbf{J}(\Psi^*)]^T \frac{\mathbf{N}}{r_m^2} \mathbf{J}(\Psi^*)\} \delta\ddot{\Psi} + \{[\mathbf{J}(\Psi^*)]^T \frac{\mathbf{K}_m \mathbf{R}^{-1} \mathbf{K}_m}{r_m^2} \mathbf{J}(\Psi^*) \\ + [\mathbf{J}(\Psi^*)]^T \frac{\mathbf{K}_m \mathbf{R}^{-1} \mathbf{H}}{r_m^2} \mathbf{J}(\Psi^*)\} \delta\dot{\Psi} + \mathbf{G}^J(\Psi^*, 0) \delta\Psi = 0 \end{aligned} \quad (3.4)$$

where $\mathbf{G}^J(\Psi^*, 0)$ is the Jacobian of $\mathbf{G}(\Psi, \dot{\Psi})$ with $\Psi = \Psi^*$, $\dot{\Psi} = 0$. Note that

$$\text{Jacobian of } \mathbf{G}(\Psi, \dot{\Psi}) \Big|_{\Psi=\Psi^*, \dot{\Psi}=0} = [\mathbf{G}^J(\Psi, \dot{\Psi}) \quad | \quad \mathbf{G}'^J(\Psi, \dot{\Psi})] \Big|_{\Psi=\Psi^*, \dot{\Psi}=0} = [\mathbf{G}^J(\Psi^*, 0) \quad | \quad 0]$$

since $\mathbf{G}'^J(\Psi^*, 0) = 0$.

Hence the closed loop system is locally stable if $\mathbf{G}^J(\Psi^*, 0)$ is positive definite and $h_1 > -k_m$, $h_2 > -k_m$.

3.3. CASE II Closed Loop Model

Suppose that the manipulator is in equilibrium when $\Psi = \Psi^*$. Then from eqs. (2.24) and (2.25) it follows that $u = u^*$ must satisfy

$$\mathbf{G}(\Psi^*, 0) = [\mathbf{J}(\Psi^*)]^T \frac{\mathbf{K}_m}{r_m} z^* \quad (3.5)$$

$$0 = -\mathbf{R}z^* + u^*$$

for some z^* .

The relation of u^* in terms of Ψ^* define the data table or feedforward control.

Now the closed-loop equations, based on eqs. (2.24), (2.25) and (3.1), are

$$\{\mathbf{M}(\Psi) + [\mathbf{J}(\Psi)]^T \frac{\mathbf{N}}{\tau_m^2} \mathbf{J}(\Psi)\} \ddot{\Psi} + \{\mathbf{G}(\Psi, \dot{\Psi}) + [\mathbf{J}(\Psi)]^T \frac{\mathbf{N}}{\tau_m^2} \frac{d}{dt} [\mathbf{J}(\Psi)] \dot{\Psi}\} = [\mathbf{J}(\Psi)]^T \frac{\mathbf{K}_m}{\tau_m} z$$

$$\mathbf{L} \dot{z} = -\mathbf{R}z - [\mathbf{K}_m + \mathbf{H}] \frac{\mathbf{J}(\Psi)}{\tau_m} \dot{\Psi} + u^* \quad (3.6)$$

If we define

$$\Psi = \Psi^* + \delta\Psi$$

$$z = z^* + \delta z$$

Then the linear perturbational equations can be obtained as

$$\{\mathbf{M}(\Psi^*) + [\mathbf{J}(\Psi^*)]^T \frac{\mathbf{N}}{\tau_m^2} \mathbf{J}(\Psi^*)\} \delta \ddot{\Psi} + \mathbf{G}^J(\Psi^*, 0) \delta \dot{\Psi} = [\mathbf{J}(\Psi^*)]^T \frac{\mathbf{K}_m}{\tau_m} \delta z \quad (3.7)$$

$$\mathbf{L} \delta \dot{z} = -\mathbf{R} \delta z - [\mathbf{K}_m + \mathbf{H}] \frac{\mathbf{J}(\Psi^*)}{\tau_m} \delta \dot{\Psi}$$

Hence the closed-loop system can be shown to be locally stable if $\mathbf{G}^J(\Psi^*, 0)$ is positive definite and $h_1 > -k_m$, $h_2 > -K_m$.

3.4. CASE III Closed Loop Model

Suppose it is desired that the manipulator be in equilibrium when $\Psi = \Psi^*$. Then from eq. (2.26) it follows that $u = u^*$ must satisfy

$$\mathbf{G}(\Psi^*, 0) - \tau_m [\mathbf{J}(\Psi^*)]^T \mathbf{K}^c \Theta^* + [\mathbf{J}(\Psi^*)]^T \mathbf{K}^c \Lambda(\Psi^*) = 0 \quad (3.8)$$

$$\tau_m^2 \mathbf{K}^c \Theta^* - \tau_m \mathbf{K}^c \Lambda(\Psi^*) = \mathbf{K}_m \mathbf{R}^{-1} u^*$$

for some Θ^* .

Again the relations of u^* in terms of Ψ^*, Θ^* define the data table in the closed-loop control.

According to eqs. (2.26) and (3.1), the closed-loop equations can be obtained as

$$\mathbf{M}(\Psi) \ddot{\Psi} + \mathbf{G}(\Psi, \dot{\Psi}) - \tau_m [\mathbf{J}(\Psi)]^T \mathbf{K}^c \Theta + [\mathbf{J}(\Psi)]^T \mathbf{K}^c \Lambda(\Psi) = 0 \quad (3.9)$$

$$\mathbf{N} \ddot{\Theta} + [\mathbf{K}_m \mathbf{R}^{-1} \mathbf{K}_m + \mathbf{K}_m \mathbf{R}^{-1} \mathbf{H}] \dot{\Theta} + \tau_m^2 \mathbf{K}^c \Theta - \tau_m \mathbf{K}^c \Lambda(\Psi) = \mathbf{K}_m \mathbf{R}^{-1} u^*$$

If we define

$$\Psi = \Psi^* + \delta\Psi$$

$$\Theta = \Theta^* + \delta\Theta$$

Then the linear perturbational equations can be obtained as

$$\mathbf{M}(\Psi^*)\delta\ddot{\Psi} + [\mathbf{G}^J(\Psi^*, 0) + \mathbf{D}(\Psi^*)]\delta\dot{\Psi} - r_m [\mathbf{J}(\Psi^*)]^T \mathbf{K}^c \delta\Theta = 0 \quad (3.10)$$

$$\mathbf{N}\delta\ddot{\Theta} + [\mathbf{K}_m \mathbf{R}^{-1} \mathbf{K}_m + \mathbf{K}_m \mathbf{R}^{-1} \mathbf{H}]\delta\dot{\Theta} + r_m^2 \mathbf{K}^c \delta\Theta - r_m \mathbf{K}^c \mathbf{J}(\Psi^*) \delta\dot{\Psi} = 0$$

where $\mathbf{D}(\Psi^*) =$ the Jacobian of $\{[\mathbf{J}(\Psi)]^T \mathbf{K}^c \Lambda(\Psi)\}$.

Hence the closed-loop system is locally stable if the matrix

$$\begin{bmatrix} \mathbf{G}^J(\Psi^*, 0) + \mathbf{D}(\Psi^*) & -r_m [\mathbf{J}(\Psi^*)]^T \mathbf{K}^c \\ -r_m \mathbf{K}^c \mathbf{J}(\Psi^*) & r_m^2 \mathbf{K}^c \end{bmatrix}$$

is positive definite and $h_1 > -K_m, h_2 > -K_m$.

3.5. CASE IV Closed Loop Model

Suppose that the manipulator is in equilibrium when $\Psi = \Psi^*$. Then from eq. (2.27) it follows that $u = u^*$ must satisfy

$$\mathbf{G}(\Psi^*, 0) - [\mathbf{J}(\Psi^*)]^T \mathbf{K}^c [r_m \Theta^* - \Lambda(\Psi^*)] = 0$$

$$r_m^2 \mathbf{K}^c \Theta^* - r_m \mathbf{K}^c \Lambda(\Psi^*) = \mathbf{K}_m z^* \quad (3.11)$$

$$0 = -\mathbf{R}z^* + u^*$$

for some Θ^* and z^* .

The relations of u^* in terms of Ψ^*, Θ^* and z^* define the data table or feedforward control.

>From eqs. (2.27) and (3.1) the closed-loop equations can be obtained as

$$\mathbf{M}(\Psi)\ddot{\Psi} + \mathbf{G}(\Psi, \dot{\Psi}) - [\mathbf{J}(\Psi)]^T \mathbf{K}^c [r_m \Theta - \Lambda(\Psi)] = 0$$

$$\mathbf{N}\ddot{\Theta} + r_m^2 \mathbf{K}^c \Theta - r_m \mathbf{K}^c \Lambda(\Psi) = \mathbf{K}_m z \quad (3.12)$$

$$\mathbf{L}\dot{z} = -\mathbf{R}z - (\mathbf{K}_m + \mathbf{H})\dot{\Theta} + u^*$$

If we define

$$\Psi = \Psi^* + \delta\Psi$$

$$\Theta = \Theta^* + \delta\Theta$$

$$z = z^* + \delta z$$

then the linear perturbational equations can be obtained as

$$\mathbf{M}(\Psi^*)\delta\ddot{\Psi} + [\mathbf{G}^J(\Psi^*, 0) + \mathbf{D}(\Psi^*)]\delta\dot{\Psi} - r_m [\mathbf{J}(\Psi^*)]^T \mathbf{K}^c \delta\Theta = 0$$

$$\mathbf{N}\delta\ddot{\Theta} + r_m^2 \mathbf{K}^c \delta\Theta - r_m \mathbf{K}^c \mathbf{J}(\Psi^*)\delta\dot{\Psi} = \mathbf{K}_m \delta z \quad (3.13)$$

$$\mathbf{L}\delta\dot{z} = -\mathbf{R}\delta z - (\mathbf{K}_m + \mathbf{H})\delta\dot{\Theta}$$

Hence the closed-loop system can be shown to be locally stable if the matrix

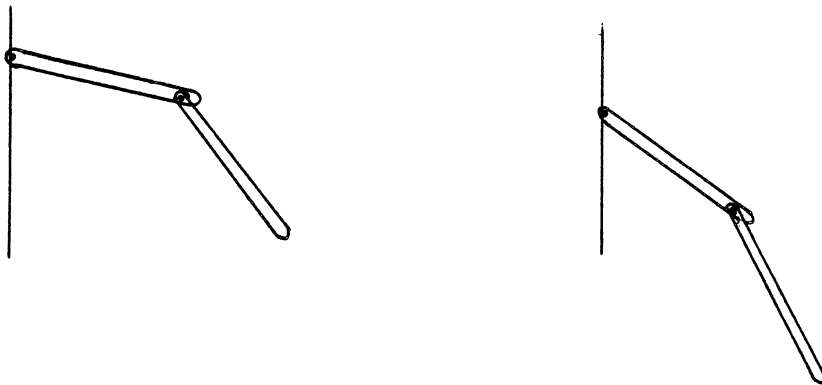
$$\begin{bmatrix} \mathbf{G}^J(\Psi^*, 0) + \mathbf{D}(\Psi^*) & -r_m [\mathbf{J}(\Psi^*)]^T \mathbf{K}^c \\ -r_m \mathbf{K}^c \mathbf{J}(\Psi^*) & r_m^2 \mathbf{K}^c \end{bmatrix}$$

is positive definite and $h_1 > -K_m$, $h_2 > -K_m$.

The previous discussion reveals that local stability of the closed loop system is achieved by nonnegative feedback gains. Because of the complicated nonlinearity, the global stability conditions for the nonlinear closed-loop system, generally, can't be obtained.

3.6. Simulation Results

The open loop system has been programmed in Fortran by using the IMSL subrouting DGEAR and simulated on the Amdahl 5860. The parameter values used in the simulation are listed in Appendix. Two final positions are considered, one is $(\psi_1, \psi_2) = (60^\circ, 30^\circ)$, the other is $(\psi_1, \psi_2) = (30^\circ, 20^\circ)$. Their corresponding arm configurations can be found as



The former final position is used for each case; however, the latter final position is only used in the elastic cables case. Corresponding to the four assumed cases, the time responses for the link angles in each case are plotted in the following.

Some features of the system are also observed from the simulation results:

- 1) The motor inductance effects are not important.
- 2) If the cables are inelastic the system is open loop stable. The region of local stability is large.
- 3) Provided the cables are elastic, the system is very sensitive. The region of local stability is essentially small. For example, in Fig 3.6 and Fig 3.7, the responses tend very slowly toward the equilibrium, the stable region is about 2° in contrast to about 45° for inelastic cables cases.
- 4) In order to properly control an elastic cable-drive system, another more complicated control strategy should be used instead of using simple displacement control.

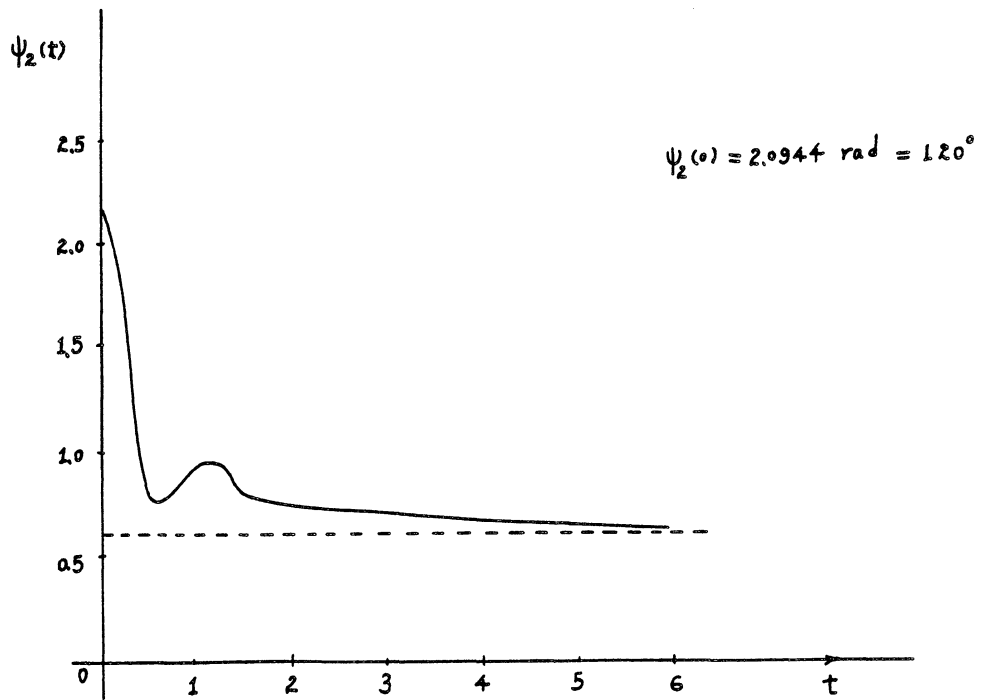
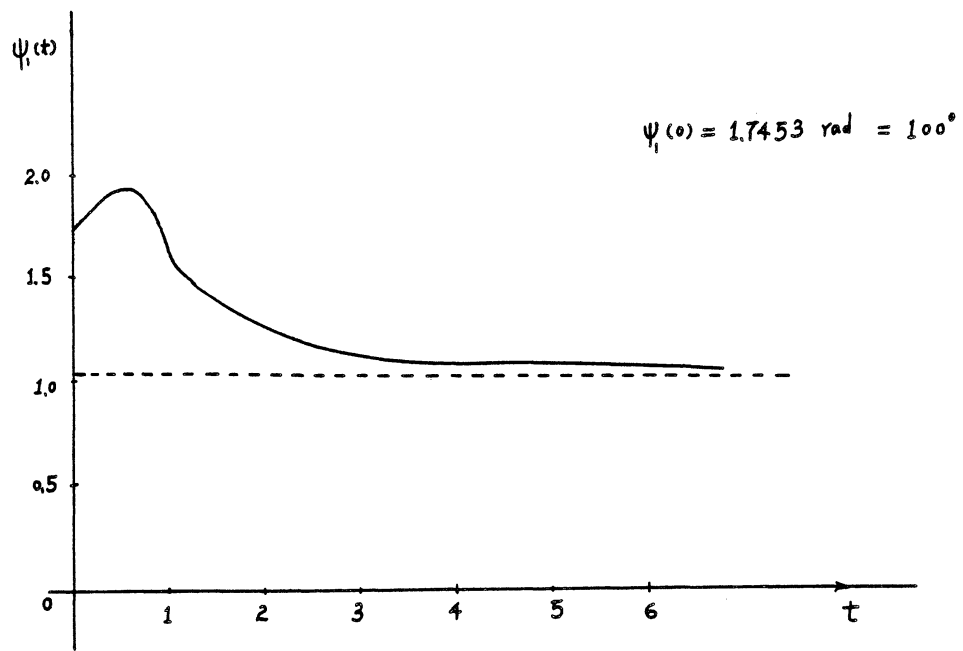


Fig 3.2 CASE I Inelastic Cables Without Motor Inductances ($h_1=h_2=0$)

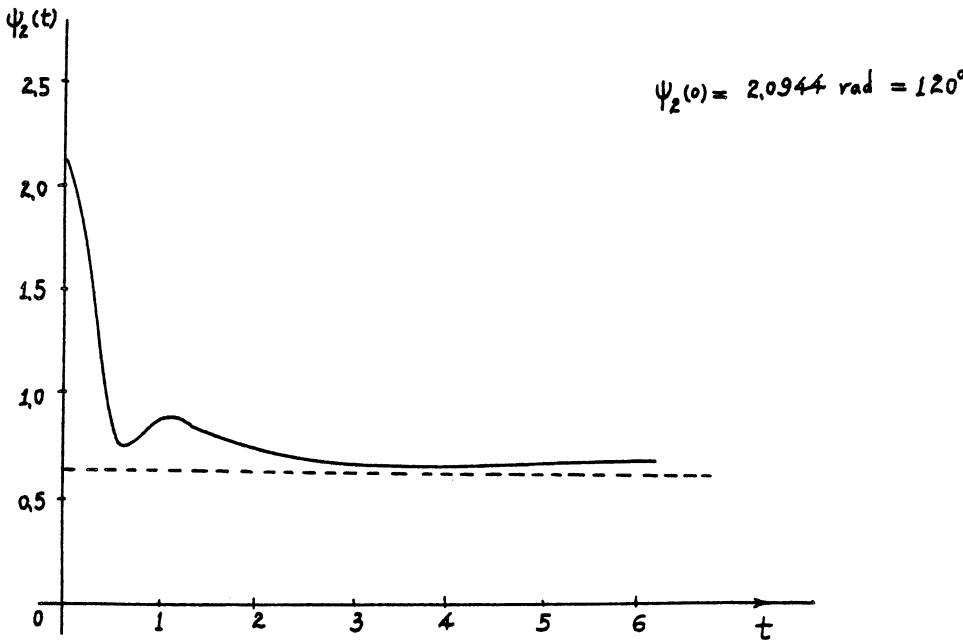
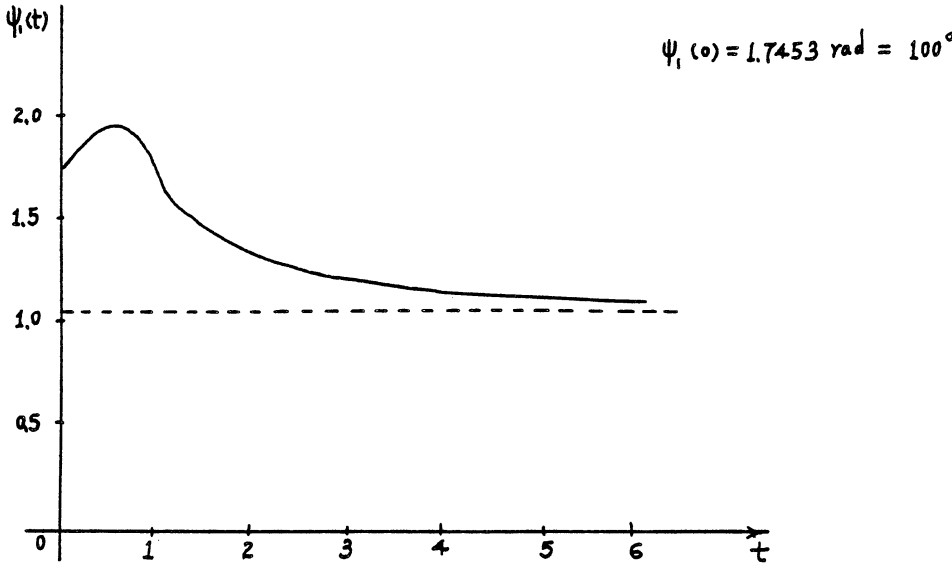


Fig 3.3 CASE II Inelastic Cables With Motor Inductances ($h_1=h_2=0$)

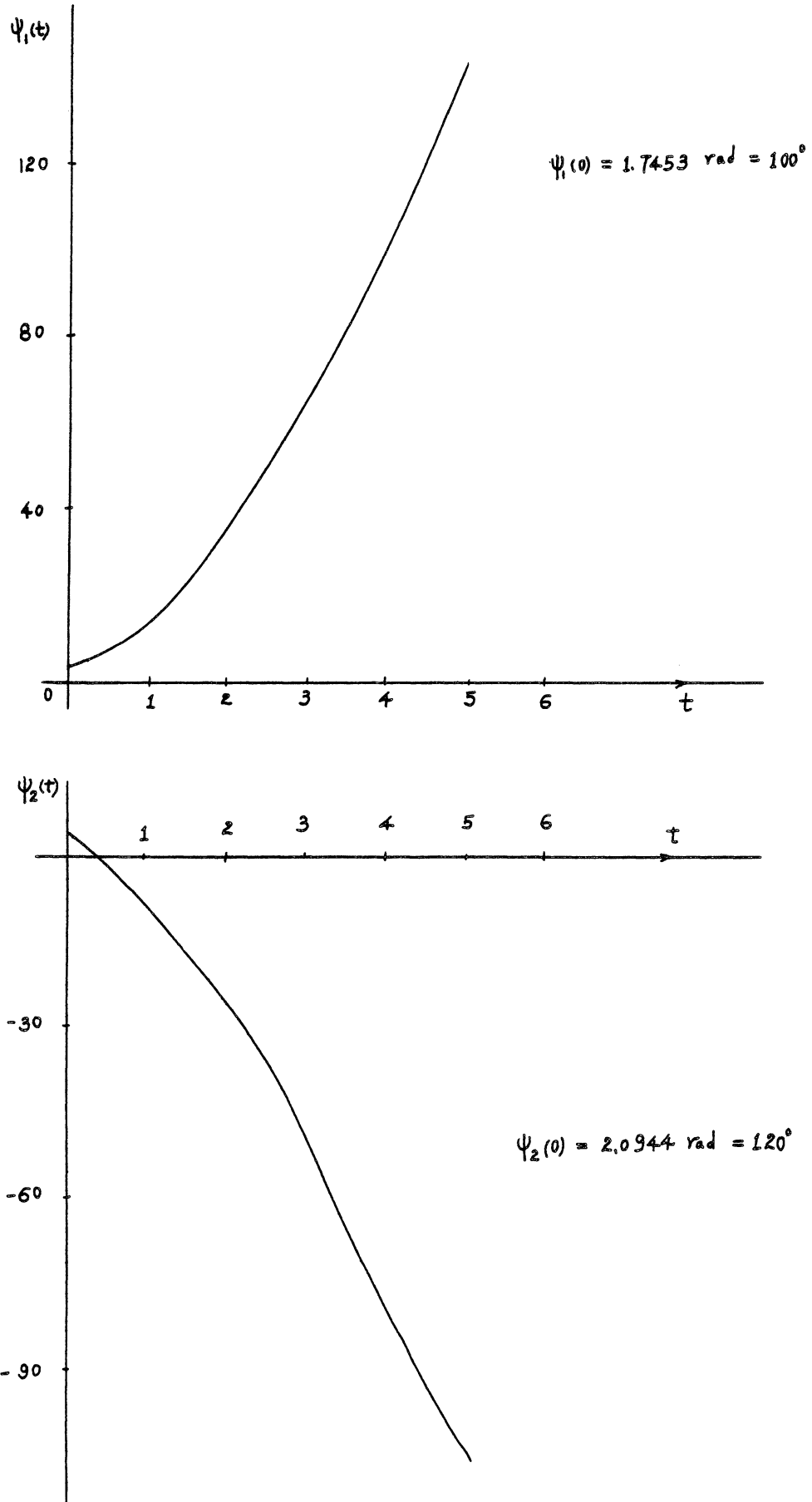


Fig 3.4 CASE III Elastic Cables Without Motor Inductances ($h_1=h_2=0$)

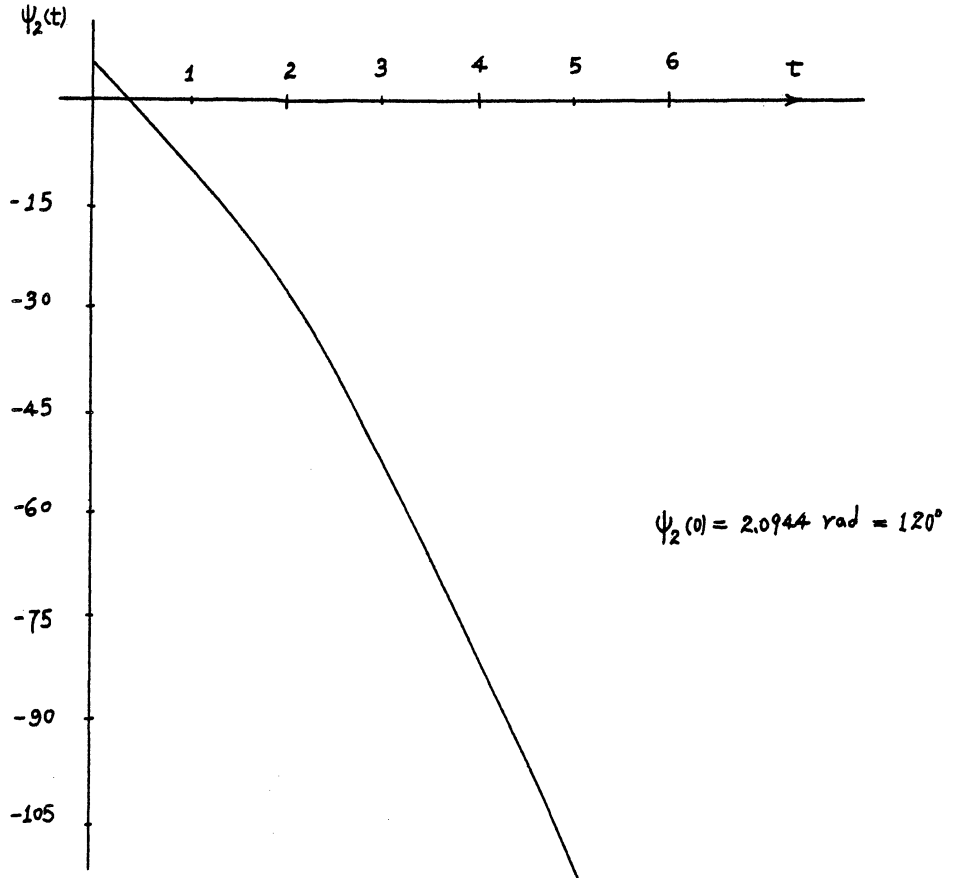
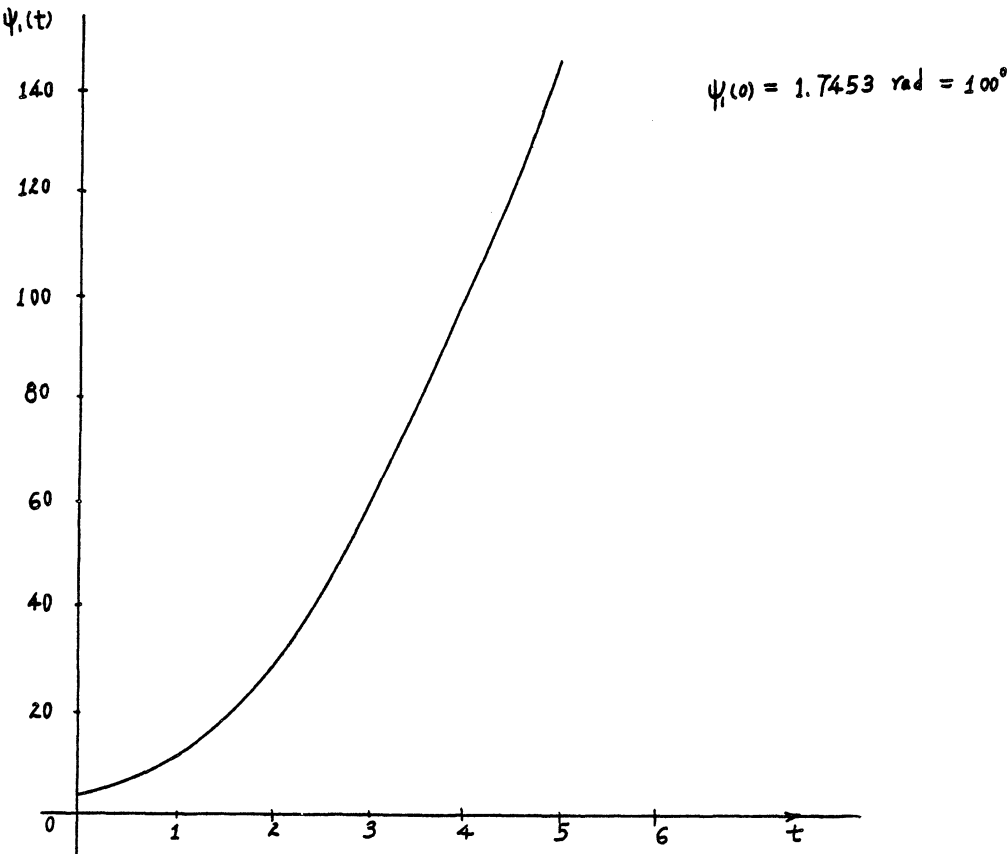


Fig 3.5 CASE IV Elastic Cables With Motor Inductances ($h_1=h_2=0$)

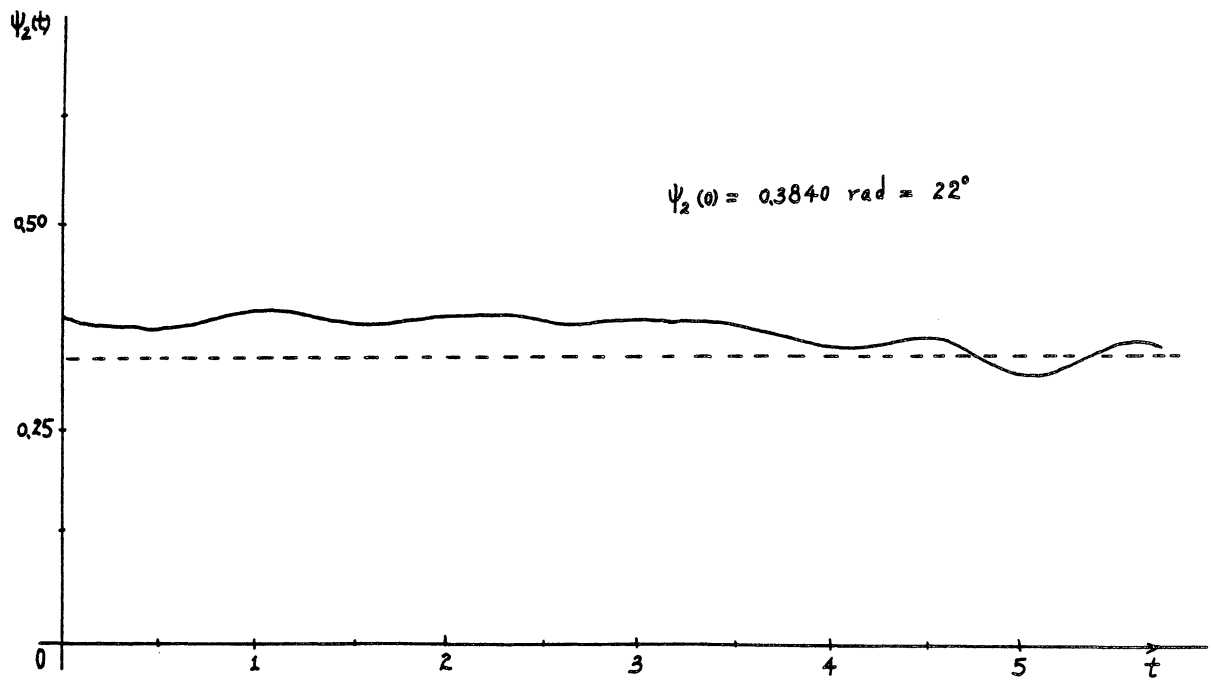
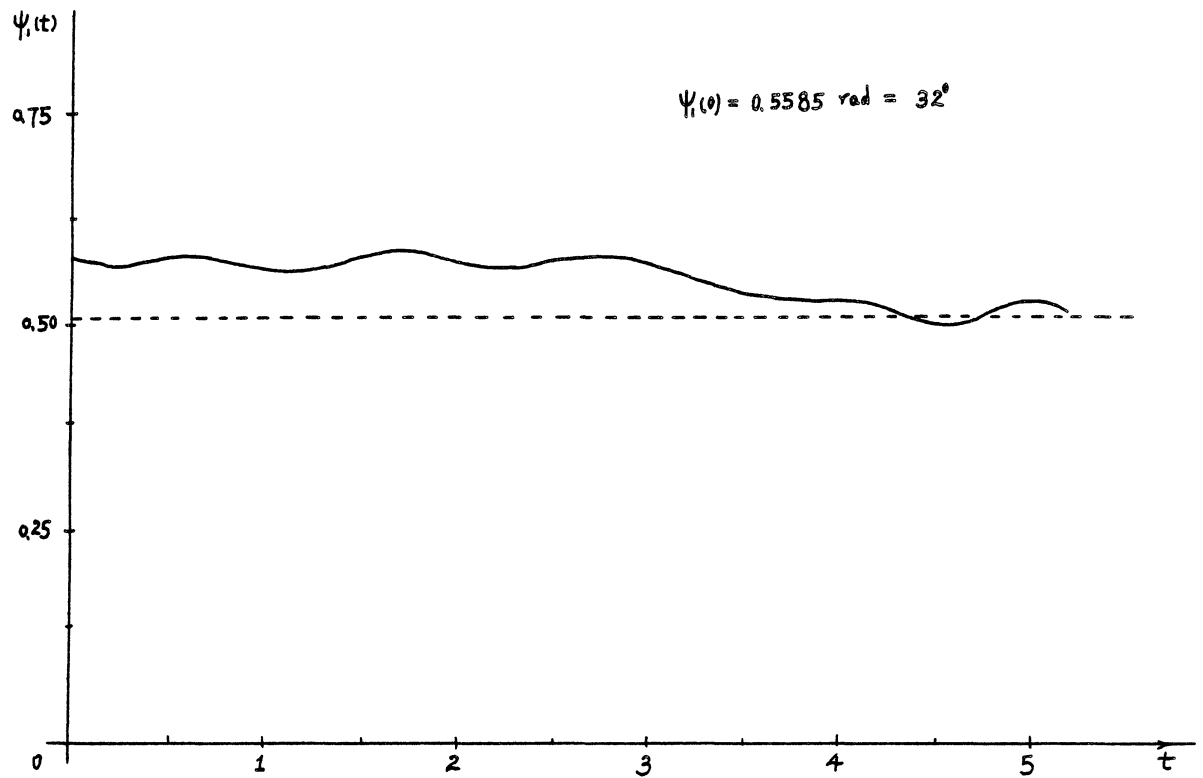


Fig 3.6 CASE III Elastic Calbes Without Motor Inductances ($h_1=h_2=0$)

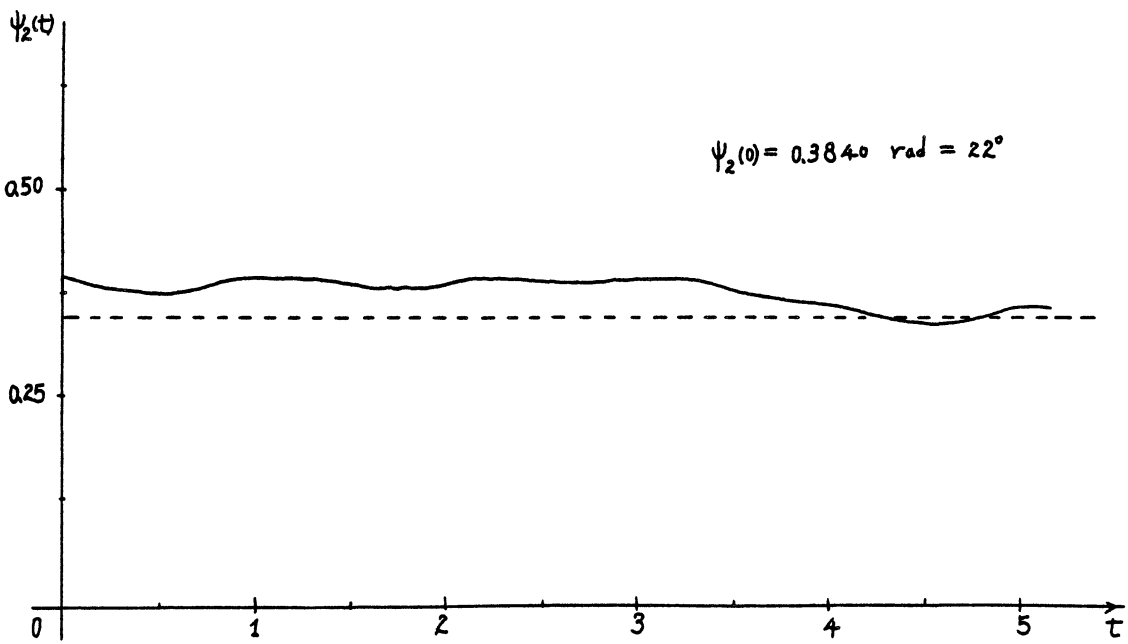
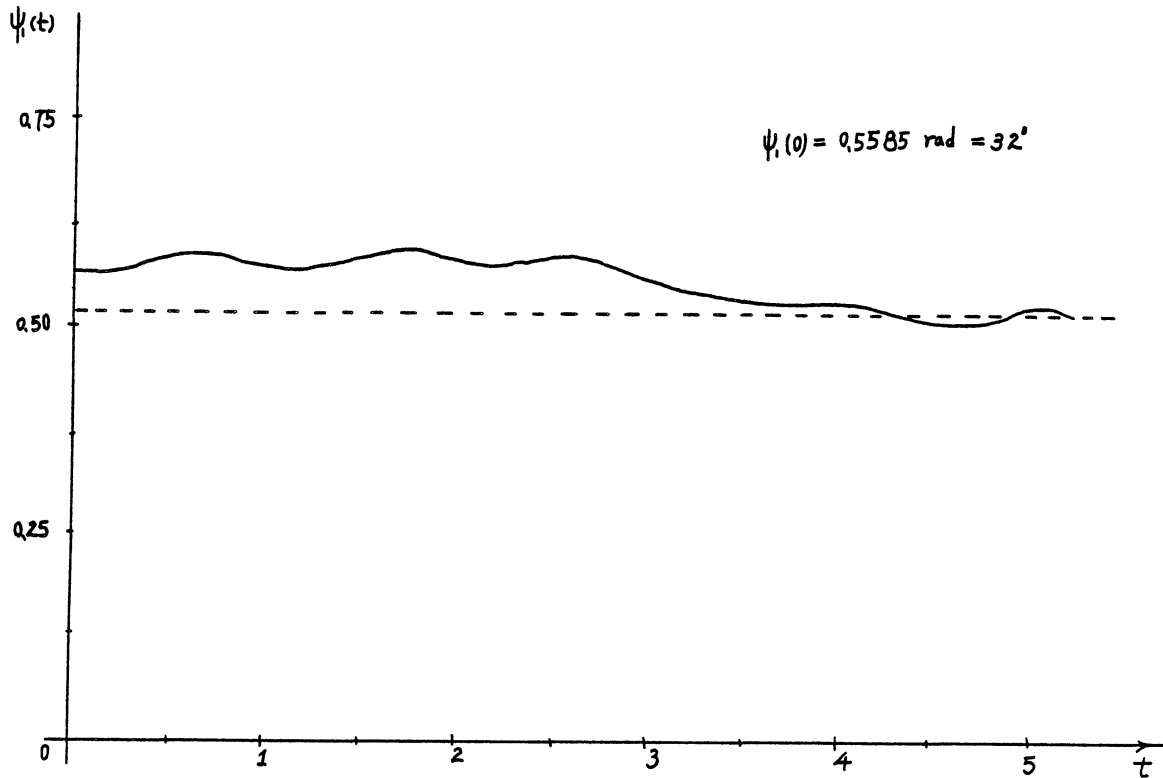


Fig 3.7 CASE IV Elastic Cables With Motor Inductances ($h_1=h_2=0$)

4. CONCLUSIONS

4.1. Summary

In this work, a mathematical model describing the dynamics of a tendon cable manipulator has been developed. From this we investigated four different cases corresponding to various assumptions about the effects of cable elasticities and motor inductances. Since the objective is final position control, the inverse kinematic problem is not considered. Open loop performance of the system is simulated on computer. The simulation results show that motion of the manipulator is not satisfactory when the cables are elastic. Table 4.1 is a list of state variables required for the four different cases. Generally, the time constant of electrical system is much smaller than that in mechanical system (by a factor about 50). That is why most people don't model the motor inductance effects, our conclusions also validate the insignificance of the motor inductance effects. However, the elasticity of cables introduces some flexibility to the tendon cable system, which seems to have a destabilizing effect.

Tendon Cables	Motor		Ignore Motor Inductances	Include Motor Inductances
	State Variables	Variables		
Inelastic			$\psi_1, \dot{\psi}_1, \psi_2, \dot{\psi}_2$ (4 th order)	$\psi_1, \dot{\psi}_1, \psi_2, \dot{\psi}_2$ i_1, i_2 (6 th order)
Elastic			$\psi_1, \dot{\psi}_1, \psi_2, \dot{\psi}_2, \vartheta_1, \dot{\vartheta}_1$ $\vartheta_2, \dot{\vartheta}_2$ (8 th order)	$\psi_1, \dot{\psi}_1, \psi_2, \dot{\psi}_2, \vartheta_1, \dot{\vartheta}_1$ $\vartheta_2, \dot{\vartheta}_2, i_1, i_2$ (10 th order)

Table 4.1

4.2. Future Work

There are a few directions that could be pursued:

- (1) Implement a controller by using more elegant strategy, such as adaptive control [15], resolved motion control [16,17] or minimum time control [2].
- (2) Use two antagonistic actuators per link [1,2,12]. This will increase the geometric complexity, however, it is more powerful, in some sense, than the configurations considered.
- (3) Extend this system to higher degree of freedom manipulator, and compare the motion capability with other typical robot structures.

5. APPENDIX

Values of the Parameters Used in the Simulations

Link Parameters

$$\begin{array}{ll}
 q_a = 0.04m & \bar{l}_{a1} = 0.3m \\
 d = 0.04m & \bar{l}_{b1} = 0.3m \\
 r_a = 0.3m & \bar{l}_{a2} = 0.28m \\
 r_b = 0.3m & \bar{l}_{b2} = 0.28m \\
 M_a = 1Kg & k_a = 350.252nt / m \\
 M_b = 1Kg & k_b = 3502.52nt / m \\
 m_a = 0.5Kg & k_a^c = 3502.52nt / m \\
 m_b = 0.5Kg & g = 9.8m / sec^2
 \end{array}$$

Motor Parameters

$$\begin{array}{ll}
 r_m = 0.015m & J_m = 4.64 \times 10^{-4} Kg - m^2 \\
 K_m = 0.394Nm / A & L_m = 5 \times 10^{-3} H \\
 R_m = 2.5r
 \end{array}$$

6. REFERENCES

- (1) Riemenschneider, P.R.H.; Johnson, T.L.; Lim, K.H.; "Final-Position Control of a Single Degree-of-Freedom Tendon Arm," *Proc. IEEE Conf. on Decision and Control*, Albuquerque, Dec. 1980.
- (2) Lim, K.H.; "Control of a Tendon Arm," S.M. Thesis, MIT, 1981.
- (3) Bejczy, A.K.; "Robot Arm Dynamics and Control," CIT JPL Technical Memo 33-669, 1974.
- (4) Luh, J.Y.S.; "Conventional Controller Design for Industrial Robots - A Tutorial," *IEEE Trans. on Systems, Man, and Cybernetics*, vol. SMC-13, no. 3, May/June 1983.
- (5) Paul, R.P.; "Robot Manipulators," MIT Press, 1981.
- (6) Benhabib, R.J.; Iwens, R.P.; and Jackson, R.L.; "A Stability of Distributed Control for Large Flexible Structures," *AIAA Guidance and Control Conf.*, Aug. 1979, pp. 79-1780.
- (7) Wu, C.H.; Paul, R.P.; "Manipulator Compliance Based on Joint Torque Control," *IEEE Conf. on Decision and Control*, 1980.
- (8) Whitney, D.E.; "Force Feedback Control of Manipulator Fine Motions," *Proc. IEEE Joint Automatic Control Conf.*, 1976, pp. 687-693.
- (9) Dombre, E.; Liegeois, A.; Borrel, P.; "Modelling the Elastic Transmissions of a Computer-Controlled Manipulator," *Proc. IEEE Joint Automatic Control Conf.*, 1980.
- (10) Khalil, W.; Liegeois, A.; "The Dynamics of a Class of Electrically-Actuated and Cable-Driven Manipulators," *Proc. of Dynamics of Multibody Systems, IUTAM Symp.* Munich, 1977.
- (11) McClamroch, N.H.; "State Models of Dynamic Systems," Springer-Verlag, 1980.
- (12) Boykin, Jr., W.H.; "A New Antagonistic Actuator for Robot Control," *IEEE Conf. on Decisions and Control*, 1982.
- (13) LeQuoc, S.; Cheng, R.M.H.; "Analysis of a Pneumatically Coupled Cam-Actuated Mechanism," *ASME Trans. J. of Dynamic Systems, Measurement, and Control*, vol. 103, Sep. 1981.
- (14) Brady, M., et al.; "Robot Motion," MIT Press, 1982.
- (15) Chung, M.J.; "Adaptive Control of a Mechanical Manipulator," Ph.D. dissertation, *University of Michigan*, Ann Arbor, Michigan, July 1983.
- (16) Wu, C.H.; Paul, R.P.; "Resolved Motion Force Control of Robot Manipulator," *IEEE Trans. on Systems, Man, and Cybernetics*, vol. SMC-12, no. 3, May/June 1982.
- (17) Lee, C.S.G., Lee B.H.; "Resolved Motion Adaptive Control for Mechanical Manipulators," CRIM Report, *University of Michigan*, Ann Arbor, Michigan, June 1983.
- (18) Luh, J.Y.S., Walker, M.W., Paul, R.P.C., "On-Line Computational Scheme for Mechanical Manipulators," *ASME J. of Dynamic Systems, Measurement and Control*, vol. 102, June 1980.
- (19) McClamroch N.H.; "Control of Large Space Structures Using Electro Mechanical Actuators," Report CSDL-p-1607 *C.S. Draper Lab Inc.*, Cambridge, Massachusetts.